ACS APPLIED MATERIALS & INTERFACES
Forum Article
www.acsami.org

Dielectric and Other Properties of Polyimide Aerogels Containing Fluorinated Blocks

Mary Ann B. Meador,*[,†] Emily McMillon,[‡] Anna Sandberg,[‡] Elizabeth Barrios,[‡] Nathan G. Wilmoth,[§] Carl H. Mueller,[⊥] and Félix A. Miranda[†]

[†]NASA Glenn Research Center, 21000 Brookpark Road, Cleveland, Ohio 44135, United States
[‡]NASA intern
[§]Vantage Partners, LLC
[⊥]Qinetiq NA

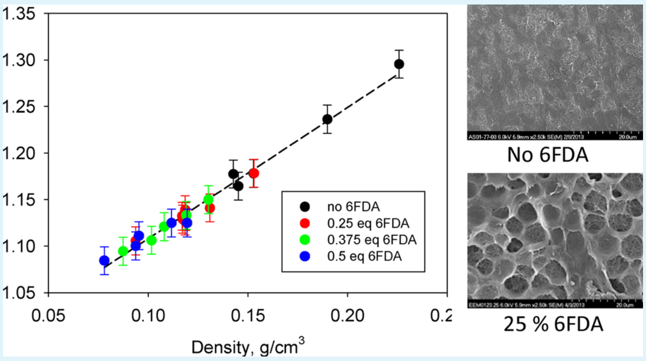

ABSTRACT: The dielectric and other properties of a series of low-density polyimide block copolymer aerogels have been characterized. Two different anhydride-capped polyimide oligomers were synthesized: one from 2,2-bis(3,4-dicarboxyphenyl)hexafluoropropane dianhydride (6FDA) and 4,4′-oxidianiline (ODA) and the other from biphenyl-3,3′,4,4′-tetracarboxylic dianhydride and ODA. The oligomers were combined with 1,3,5-triaminophenoxybenzene to form a block copolymer networked structure that gelled in under 1 h. The polyimide gels were supercritically dried to give aerogels with relative dielectric constants as low as 1.08. Increasing the amount of 6FDA blocks by up to 50% of the total dianhydride decreased the density of the aerogels, presumably by increasing the free volume and also by decreasing the amount of shrinkage seen upon processing, resulting in a concomitant decrease in the dielectric properties. In this study, we have also altered the density independent of fluorine substitution by changing the polymer concentration in the gelation reactions and showed that the change in dielectric due to density is the same with and without fluorine substitution. The aerogels with the lowest dielectric properties and lowest densities still had compressive moduli of 4−8 MPa (40 times higher than silica aerogels at the same density), making them suitable as low dielectric substrates for lightweight antennas for aeronautic and space applications.

KEYWORDS: *aerogels, polyimides, low dielectric, antennas, mesoporous*

■ INTRODUCTION

Materials with low relative dielectric constants are of great interest for high-performance electronic devices.[1] Strategies to making ultralow-dielectric materials that access dielectric constants below 2.5 typically introduce nanopores to reduce the density. For example, silica and organic (resorcinolformaldehyde and melamineformaldehyde) aerogels have been measured with dielectric constants as low as 1.008 (density = 0.008 g/cm^3),[2] but these aerogels tend to be very brittle and prone to cracking. The development of a stronger, ultralow-dielectric material with controlled porosity is considered to be essential for use in high-performance electronic devices because the materials need to resist cracking in service and survive demanding processing steps such as polishing, bonding, dicing, and cutting.[1]

Recently, we have reported the dielectric properties for polyimide aerogels with an emphasis on using them as lightweight, low-dielectric substrates for antennas.[3] In the study, relative dielectric constants as low as 1.16 were measured in the X-band frequency range for polyimide aerogels with densities on the order of 0.11 g/cm^3. In addition, it was found that dielectric constants varied linearly with the density for the polyimide aerogels, similar to silica and organic aerogels previously measured. By using the low-density, low-dielectric polyimide aerogel as a substrate in a simple, microstrip patch antenna, we also demonstrated higher gain, wider bandwidth, and lower mass compared to typical antenna substrates. These results could lead to a decrease in the weight and complexity of antenna systems, especially aboard aircraft, by reducing both the number and weight of the antennas.[4,5]

In general, the dielectric properties decrease with the density for porous polyimides made in different ways, such as the incorporation of porous fillers,[6,7] use of photochemically[8] or thermally[9] labile blocks, or foaming.[10] However, the lowest density and dielectric properties were achieved, as previously

Special Issue: Applications of Hierarchical Polymer Materials from Nano to Macro

Received: November 13, 2013
Accepted: January 15, 2014
Published: January 31, 2014

mentioned, using the approach of making polyimide aerogels cross-linked with 1,3,5-triaminophenoxybenzene (TAB).[3]

Other recent studies show that the use of fluorinated monomers in a polyimide backbone can reduce the dielectric properties of polyimides even more. For example, Othman et al.[11] made porous polyimides by acid etching a silica phase. While the relative dielectric constant decreased with increasing porosity, it was further reduced by the incorporation of hexafluoroisopropylidene groups in the polyimide backbone. Ronova et al.,[12] Simpson and St. Clair,[13] Hougham et al.,[14] and others also showed that the presence of fluorinated groups slightly decreased the relative dielectric constant, attributing this to an increase in the free volume and lower polarizability of the fluorines. Another recent study discussed the fabrication of polyimides containing polyhedral oligomeric silsesquioxanes with fluorinated side chains.[15] In the study, relative dielectric constants decreased from 3.2 to 2.3 with the addition of 15% of these side groups, while the bulk density went from 1.37 to 1.02 g/cm^3. The decrease in the dielectric constant was suggested to be due to a combination of higher free volume, as well as the lower polarizability and greater hydrophobicity of the fluorine groups, but it is not clear from these studies which of these factors plays a larger role.

In this paper, we examined the effect of increasing the amount of 2,2-bis(3,4-dicarboxyphenyl)hexafluoropropane dianhydride (6FDA) in the backbone of the polyimide aerogels on the dielectric properties. Mechanical properties, such as Young's modulus, compressive strength, or tensile strength, within an aerogel family are typically correlated to the density and tend to decrease with decreasing density. For example, Young's modulus, E_y, for silica aerogels at varying density, σ, follows a scaling law where E_y, is proportional to σ^γ, where $\gamma = 3.7$.[16] Mechanical properties of polyimide aerogels also, in general, decrease with decreasing density, although the rigidity of the polymer backbone also plays a role, with a more rigid backbone having a higher modulus at lower density than a more flexible backbone.[3] If by including fluorination in the backbone the dielectric constant could be reduced further without decreasing the density, it may be possible to maintain better mechanical properties. The aerogels were fabricated as shown in Scheme 1. In the scheme, 6FDA and biphenyl-3,3′,4,4′-tetracarboxylic dianhydride (BPDA) were used in combination to make the aerogels but were reacted separately with 4,4′-oxidianiline (ODA) to create two different oligomer blocks. The oligomers were combined with TAB to form cross-linked polyamic acids, which were chemically imidized at room temperature to form polyimide gels. The gels were dried using supercritical CO$_2$ extraction to yield the aerogels. Dielectric, physical, and mechanical properties of the aerogel formulations were characterized and compared in the study.

■ EXPERIMENTAL SECTION

Materials. 1,3,5-Triaminophenoxybenzene (TAB) was obtained from Triton Systems (200 Turnpike Road No. 2, Chelmsford, MA 01824-4053). Pyridine, acetic anhydride, and anhydrous *N*-methylpyrrolidinone (NMP) were purchased from Sigma Aldrich. 4,4′-Oxydianiline (ODA), 2,2-bis(3,4-dicarboxyphenyl)hexafluoropropane dianhydride (6FDA), and biphenyl-3,3′,4,4′-tetracarboxylic dianydride (BPDA) were obtained from Chriskev, Inc. (13920 West 108th Street, Lenexa, KS 66215). Dianhydrides were dried at 125 °C in vacuum for 24 h before use. All other reagents were used without further purification.

Scheme 1. Synthesis of Polyimide Block Copolymer Aerogels with TAB Cross-links

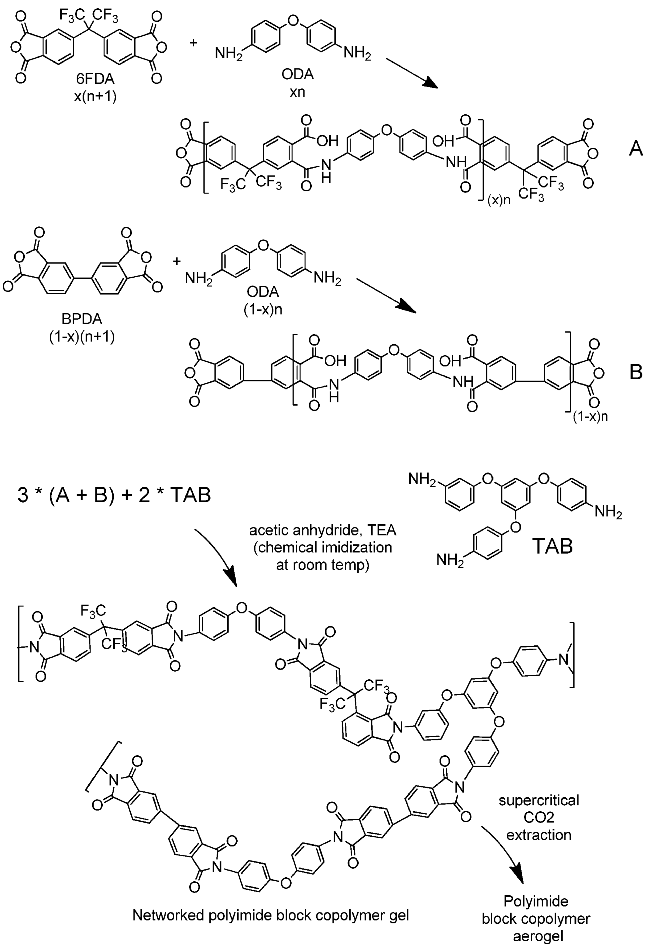

Synthesis of Polyimide Aerogels Using Chemical Imidization. Polyimide aerogels were prepared according to a procedure previously described[17] except that, as shown in Scheme 1, two dianhydrides, 6FDA and BPDA, were used. Because of the much poorer reactivity of 6FDA compared to BPDA, to achieve gelation, the two dianhydrides were separately reacted with the diamine ODA and then combined in one solution before the addition of TAB. Table 1 lists different formulations of aerogels made in the study using three different variables: 6FDA concentration, formulated number of repeat units in the oligomers (*n*), and total polymer concentration in solution. The dianhydride fraction is expressed in Table 1 as the fraction of 6FDA used as a function of the total (BPDA is implied to be 1 − 6FDA fraction).

As an example, the preparation of sample 16 from Table 1 is described. Two separate solutions were prepared as follows and are labeled in Scheme 1. Solution A: To a solution of 22.25 mL of NMP and 0.81 g (4.06 mmol) of ODA was added 1.89 g (4.26 mmol) of 6FDA with stirring for about 15 min until dissolved. Solution B: To a solution of 61.76 mL of NMP and 2.44 g (12.2 mmol) of ODA was added 3.76 g (12.8 mmol) of BPDA with stirring for about 15 min until dissolved. The two solutions, A and B, were combined with stirring, and a solution of 0.216 g (0.541 mmol) of TAB in 5 mL of NMP was added. After a few minutes of stirring, 12.88 mL (0.136 mol) of acetic anhydride and 2.37 mL (0.0170 mol) of triethylamine were added to the solution. Immediately after mixing, the solution was poured into prepared molds. The samples were allowed to gel and aged for 24 h before extraction into a 25% acetone/75% NMP solution. After another 24 h, the gel was exchanged into a solvent bath of a 75% acetone/25% NMP solution. Every 24 h thereafter, the solvent was exchanged to 100% acetone for a total of five washes. Finally, acetone was removed from the gels using supercritical CO$_2$ extraction, followed by overnight vacuum drying at 80 °C. The

Table 1. Properties of Polymide Aerogels in the Study

sample	*n*	6FDA, fraction	polymer concn, wt %	density, g/cm^3	shrinkage, %	porosity, %	surface area, m^2/g	dielectric constant, X band	modulus, MPa
1	20	0.000	8.5	0.153	17.2	89.4	340	1.18	20.67
2	30	0.000	10	0.190	19.5	86.7	327	1.24	36.14
3	10	0.000	10	0.226	23.9	84.2	337	1.30	36.18
4	20	0.375	8.5	0.102	10.8	93.2	374	1.11	6.07
5	20	0.375	10	0.130	10.8	91.1	389	1.15	15.51
6	30	0.375	8.5	0.119	12.3	91.8	396	1.13	6.21
7	20	0.375	7	0.087	9.0	94.2	443	1.10	8.06
8	10	0.375	8.5	0.108	8.7	92.8	400	1.12	7.42
9	30	0.000	7	0.143	20.2	89.8	372	1.18	14.78
10	10	0.000	7	0.145	20.9	89.9	362	1.17	13.22
11	20	0.500	8.5	0.095	10.2	93.2	445	1.11	6.04
12	30	0.500	7	0.094	12.2	93.5	494	1.10	5.51
13	30	0.500	10	0.112	12.2	92.6	452	1.13	3.35
14	10	0.500	10	0.120	9.5	91.9	404	1.13	3.20
15	10	0.500	7	0.078	7.7	94.7	456	1.08	4.72
16	20	0.250	8.5	0.118	11.5	92.0	366	1.13	10.63
17	20	0.250	8.5	0.117	11.5	92.0	394	1.13	15.30
18	20	0.250	8.5	0.119	11.8	92.0	343	1.14	10.52
19	20	0.250	8.5	0.119	11.3	92.3	389	1.13	20.88
20	20	0.250	10	0.153	14.6	89.6	368	1.18	24.07
21	30	0.250	8.5	0.131	13.5	91.2	382	1.14	20.47
22	20	0.250	7	0.094	11.2	94.0	402	1.11	8.57
23	10	0.250	8.5	0.117	10.7	92.3	388	1.13	9.88

resulting aerogels had a bulk density of 0.118 g/cm^3. FT-IR (δ): 1772, 1718, 1500, 1375, 1240, 1110 (br), 1082 (br). Solid ^{13}C NMR (ppm): 64.3, 125−130, 141.9, 154.4, 165.0.

Characterization. Permittivity measurements were taken using the waveguide transmission measurement technique, which has been previously described.[3,18] Compression testing of the specimens was carried out as previously described[4] in accordance with ASTM D695-10, with the sample sizes nominally 1.5−1.8 cm in diameter and 3 cm in length (close to the 1:2 ratio of diameter-to-length as prescribed for the testing of polymer foams). The samples were tested between a pair of compression plates on a model 4505 Instron load frame. The modulus was taken as the initial slope of the stress−strain curve using marks painted directly on the aerogel specimens and is reported in Table 1.

RESULTS AND DISCUSSION

Initially, it was of interest to make polyimide aerogels with 100% 6FDA in the backbone. However, because of the lower reactivity of 6FDA with amine, these formulations, even with a lower number of repeat units, did not gel reliably. Hence, as shown in Scheme 1, polyimide gels were made with a fraction of 6FDA replacing BPDA in the polyimide backbone. While gels could be made with fractions up to 0.75 equiv of 6FDA replacing BPDA using 10 repeat units and 10 wt % total polymer concentration in solution, it was also desired in this study to investigate the effect of a lower polymer concentration and higher number of repeat units, *n*. The former will probe the effect of lower density alone on aerogel properties (independent of the 6FDA content), while the latter will investigate the effect of the cross-link density. Thus, the study was limited to 0.5 equiv of 6FDA and 0.5 equiv of BPDA in the backbone, enabling *n* to be varied between 10 and 30 formulated repeat units and the weight percent of polymer in solution to be varied between 7 and 10 wt %. The formulations were prepared according to Scheme 1, where 6FDA and BPDA were reacted separately with ODA and then combined. Hence, polyimide gels with distinct fluorinated and nonfluorinated blocks should be obtained. The three-variable study (*n*, polymer concentration, and 6FDA fraction) was carried out as a statistical experimental design. Formulations in the study along with measured properties are shown in Table 1. Using multiple linear regression analysis and backward stepwise regression starting with full quadratic models, empirical models describing the effect of each variable on the measured properties were derived. Note that data were orthogonalized prior to analysis and the formulation in the middle of the design space (*n* = 20, 6FDA fraction = 0.5, polymer concentration = 8.5 wt %) was repeated five times to assess the model reliability and reproducibility.

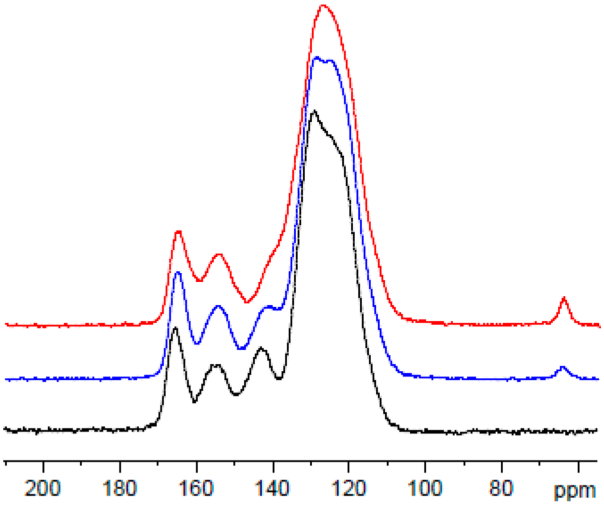

Figure 1. Solid ^{13}C NMR spectra of polyimide aerogels with (bottom), no 6FDA, (middle), 0.25 equiv of 6FDA, and (top) 0.50 equiv of 6FDA.

Characterization of the chemical structures of the aerogels was carried out using Fourier transform infrared (FT-IR) and

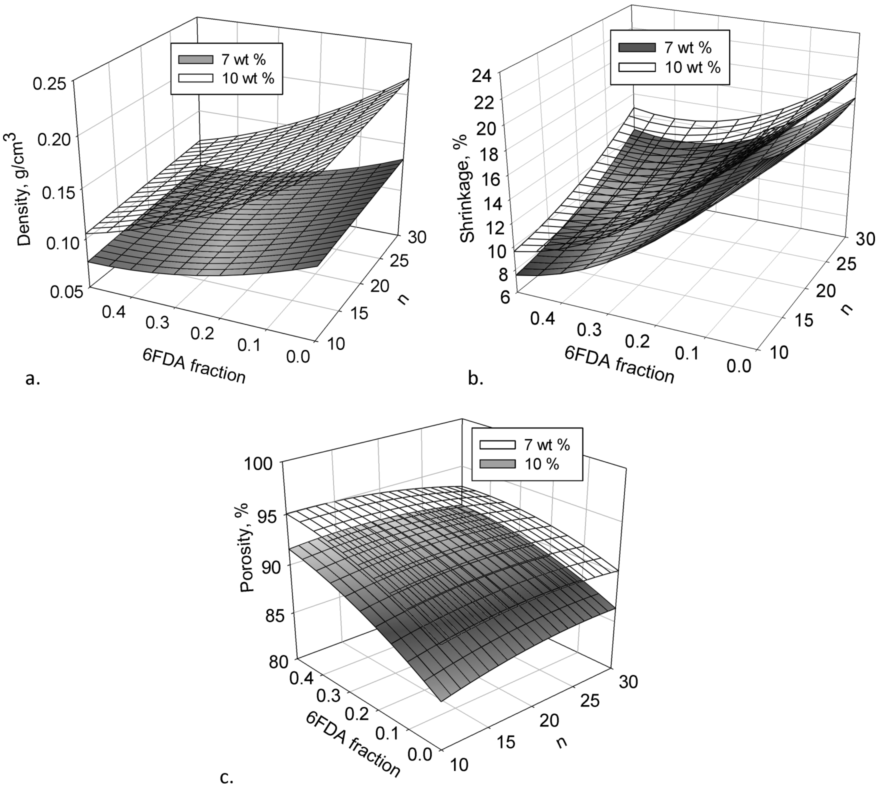

Figure 2. Empirical models for (a) density, (b) shrinkage, and (c) porosity graphed in terms of the 6FDA fraction and *n*, at two levels of solid concentration.

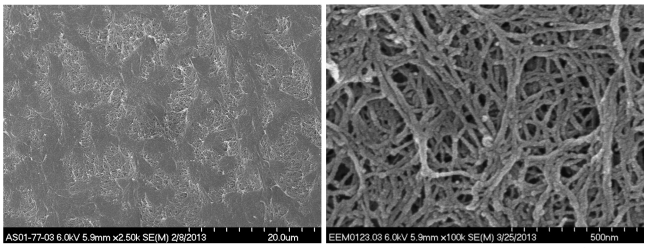

a. Sample 1 (0 6FDA, density = 0.153 g/cm^3, surface area = 340 m^2/g)

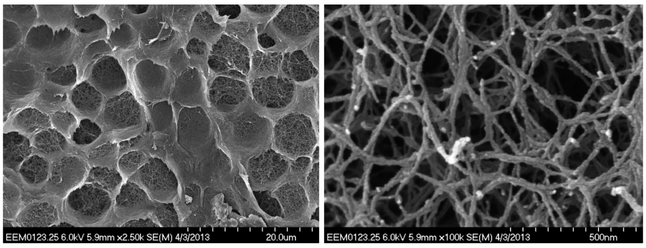

b. Sample 17 (0.25 eq 6FDA, density = 0.118 g/cm^3, surface area = 366 m^2/g)

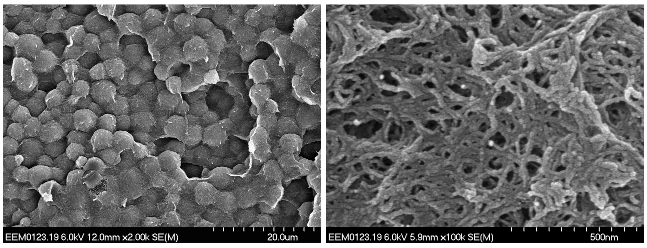

c. Sample 11 (0.5 eq 6FDA, density = 0.095 g/cm^3, surface area = 445 m^2/g)

Figure 3. SEM images of the fracture surfaces of polyimide aerogels at low (left) and high (right) magnification for (a) 6FDA fraction = 0, (b) 6FDA fraction = 0.25 equiv, and (c) 6FDA fraction = 0.5 equiv.

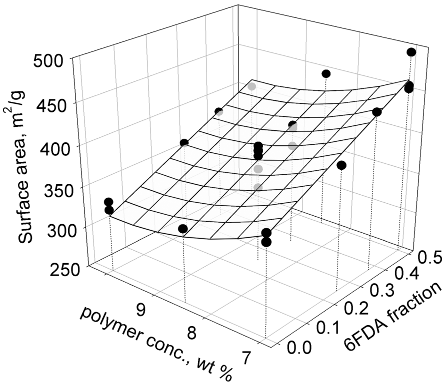

Figure 4. Empirical model for surface area versus the solid concentration and 6FDA fraction graphed with measured data points used to fit the model.

solid ^{13}C NMR spectroscopy. FT-IR of all of the aerogels showed representative peaks for imide carbonyl (1775 and 1721 cm^{-1}), a para-substituted phenyl ring of the ODA (1500 cm^{-1}), and the imide ring (1375 cm^{-1}). A comparison of solid ^{13}C NMR spectra shown in Figure 1 of three aerogel formulations made using 0, 0.25, and 0.5 equiv of 6FDA clearly shows that 6FDA is incorporated into the aerogels. All three spectra have peaks at 165 ppm (imide carbonyl), 154.4 ppm (aromatic ether from ODA and TAB), and 110−130 ppm (other aromatic peaks). The most evident difference in the spectra is the increasing peak at 64.3 ppm and the decreasing peak at 143 ppm with increasing 6FDA concentration. The peak at 64.3 ppm is due to the carbon between the two CF_3 groups and is small because it is both quaternary and split by the fluorine atoms on neighboring carbon atoms. The CF_3

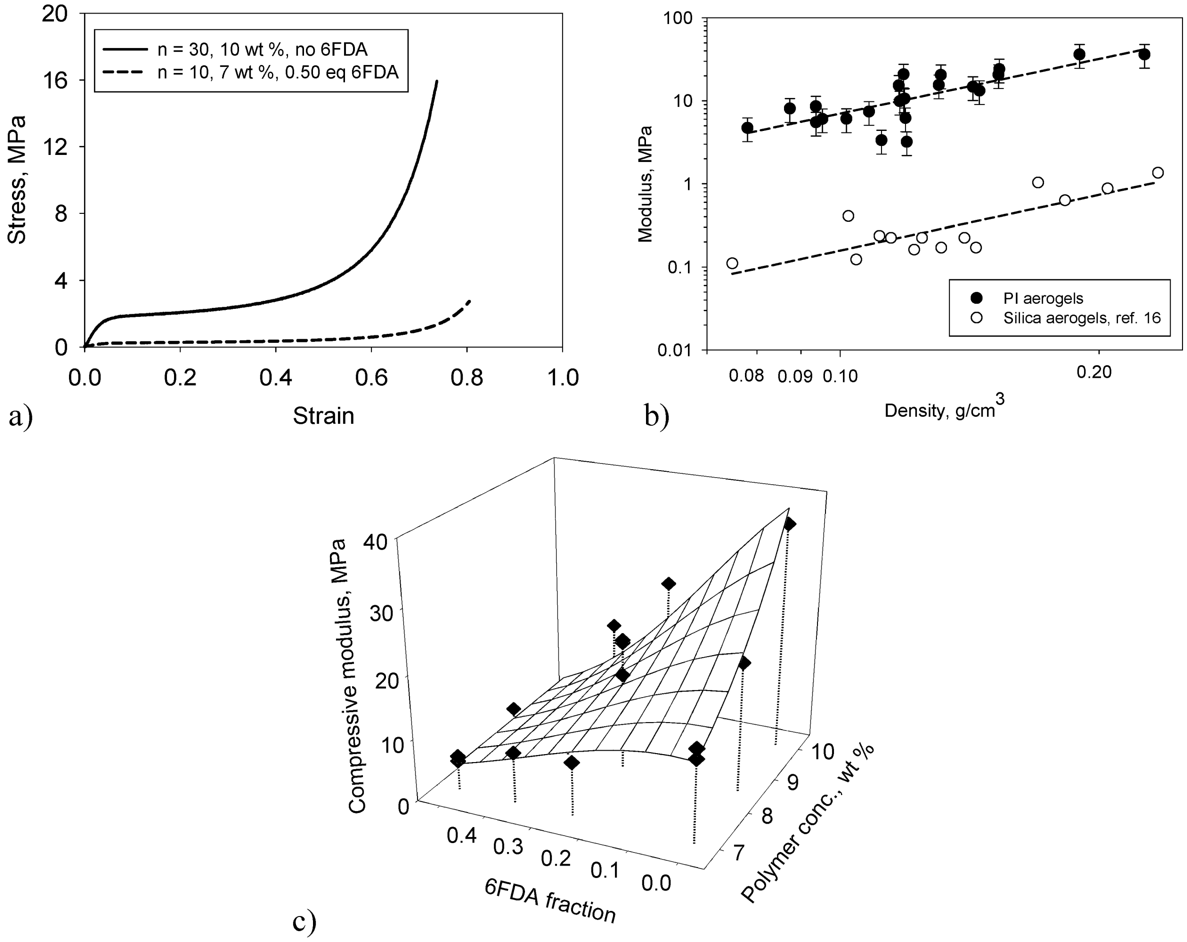

Figure 5. Graphs of (a) stress−strain curves from compression tests, (b) log modulus plotted versus log density, and (c) empirical model of the modulus from compression versus the solid concentration and 6FDA fraction shown with the measured data used to fit the model.

carbon peaks are hidden under the broad aromatic peak at 110−130 ppm. The peak at 143 ppm is due to biphenyl carbon in BPDA and should decrease as BPDA is replaced with 6FDA.

Figure 2 shows empirical models of density, shrinkage, and porosity of the aerogels in the study graphed versus the 6FDA fraction and *n*. For the empirical model of density shown in Figure 2a (standard deviation = 0.006 g/cm^3; R^2 = 0.98), it is shown that a decrease in the polymer concentration leads to decrease in the density, which was expected. The increasing fraction of 6FDA also causes a decrease in the density. This could be due to the greater free volume introduced into the aerogel by the hexafluoroisopropylidene groups, but it should be noted that 6FDA also leads to a significant decrease in shrinkage, especially when n = 10, as shown in Figure 2b (standard deviation = 0.96%; R^2 = 0.97), which also contributes to the lower density. Increasing n and decreasing the polymer concentration also significantly reduce shrinkage and density, although the effect is more subtle. Previously, we have attributed differences in shrinkage in different formulations of polyimide aerogels to solvent interactions with the polymer backbone during gelation, rigidity of the polymer chains, and interaction between chains.[13] Indeed, the larger hexafluoroisopropylidene groups would reduce the chain packing and rigidity, both of which have been shown to reduce shrinkage in other formulations of polyimide aerogels.

Porosity is calculated from the bulk density and skeletal density measured by helium pycnometry. Empirical models for porosity (standard deviation = 0.45%; R^2 = 0.98) shown in Figure 2c, as expected, show an increase in the porosity with increasing 6FDA and decreasing polymer concentration in opposition to the effects on the density and shrinkage.

The arrangement of the pores is also affected by the 6FDA concentration, as shown in scanning electron microscopy (SEM) images of the fracture surfaces in Figure 3. Figure 3a shows two different magnifications of polyimide aerogel with no 6FDA (sample 1 in Table 1). In this case, both low and high magnification display a fairly uniform arrangement of pores and polymer strands. In contrast, both parts b (sample 17, 0.25 6FDA) and c (sample 11, 0.5 6FDA) of Figure 3 reveal a hierarchical arrangement of pores and polymer chains. At lower magnification (left), micrometer-sized spherical features are displayed, while higher magnification (right) reveals that finer porosity exists inside these features and is more typically what is seen as the polymer aerogel nanostructure. The hierarchical pore structure most likely arises from macroscale phase separation of the fluorinated and nonfluorinated polymer chains during the gelation process.

The surface areas of the aerogels were measured by nitrogen sorption and analyzed using the Brunauer−Emmett−Teller (BET) method.[19] As shown in Figure 4, only the polymer concentration and 6FDA fraction are significant variables in the empirical model of surface area (standard error = 16.04 m^2/g; R^2 = 0.88), with 6FDA having the largest effect. The surface area greatly increased with increasing 6FDA fraction, further

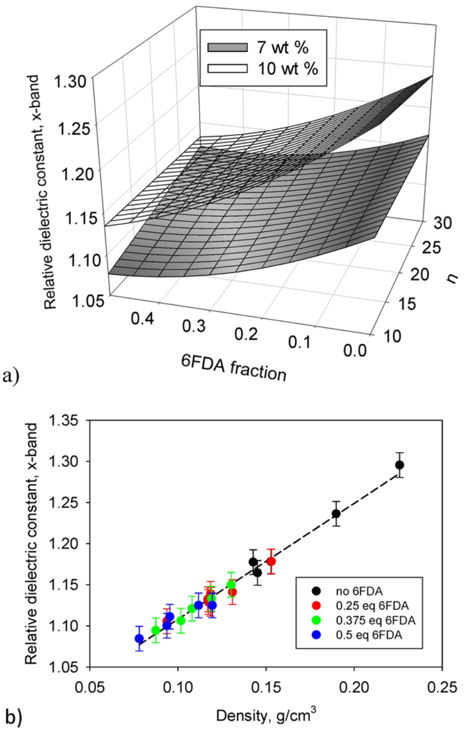

Figure 6. Graphs of (a) the empirical model of relative dielectric constant graphed versus the DMBZ fraction and *n* for two levels of solid concentration and (b) the relative dielectric constant versus density for various formulations of aerogels showing linear correlation regardless of the 6FDA concentration.

supporting the theory that the micrometer-sized features seen in the SEM images at lower magnification are filled with smaller pores. The surface area also increased with decreasing polymer concentration, consistent with the fact that lower polymer concentration leads to higher porosity and lower density. The formulated number of repeat units, *n*, did not have a significant effect on the surface area over and above standard error.

Typical stress−strain curves from compression tests of the aerogels are shown in Figure 5a. The two curves represent extremes in the study. Young's modulus was taken as the initial slope of the stress−strain curve. Typically, the modulus in aerogels is highly correlated with density. However, the plot of modulus versus density shown in Figure 5b for all of the aerogels in the study shows a somewhat loose correlation with density ($R^2 = 0.6$). We have observed this before in polyimide aerogels, where the stiffness or flexibility of the polymer backbone also affects the modulus independent of density.[13] Figure 5b also shows a comparison of the modulus with silica aerogels over the same range of density.[16] The two plots are nearly parallel and show a 40-fold increase in the modulus over the whole range.

The empirical model for modulus (log standard deviation = 0.12; $R^2 = 0.87$) is shown in Figure 5c along with the measured data points used to calculate the model. As shown, only the 6FDA fraction and polymer concentration have a significant effect on the modulus over and above the standard error. When no 6FDA is used in the aerogel, the polymer concentration has the largest effect on the modulus. The modulus increases with increasing polymer concentration, most likely because of the concomitant increase in density, more than doubling over the entire range. When the 6FDA fraction is 0.5, however, the modulus is low (3−6 MPa) across the entire range of polymer concentration due to the greater flexibility of the 6FDA-containing backbone.

The relative dielectric constants were measured in the X-band range (11−12 GHz). Figure 6a shows the empirical model of the relative dielectric constant (standard deviation = 0.012; $R^2 = 0.96$). All three variables affect the dielectric constant with the largest effect being the polymer concentration, followed by the 6FDA fraction. Interestingly, a comparison of this graph to the empirical model for density shown in Figure 2a shows the plots to be nearly identical. This strongly suggests that any impact of the variables on the dielectric constant is really the effect of the variables on the density. In fact, the plot of the relative dielectric constant shown in Figure 6b shows a strong correlation with density ($R^2 = 0.98$). Thus, the contribution to the dielectric properties from the addition of the hexafluoroisopropylidene groups to the polyimide aerogel backbone is mainly due to the larger free volume and lower shrinkage, which leads to lower density and not to other attributes of fluorination such as lower polarizability or hydrophobicity. Because the fluorinated blocks also introduce other issues, such as hierarchical pore structure, lower reactivity, and lower modulus, it may be better to use other strategies to reduce the density and relative dielectric constants.

■ CONCLUSIONS

The dielectric constant and other properties of polyimide aerogels with fluorinated and nonfluorinated blocks have been examined for possible use as a low dielectric constant substrate for antennas and other applications. Lower dielectric constant substrates potentially improve antenna gain and bandwidth, while the lower density of the aerogels reduces the weight of the antennas. A statistical experimental design was carried out to understand the effect of the increasing amount of fluorinated blocks, polymer concentration, and formulated number of repeat units, *n*, on the properties of the aerogels. The lowest relative dielectric constant (1.084) was measured for the lowest-density (0.078 g/cm^3) aerogels in the study, which were made using the lowest polymer concentration, fewest repeat units, and highest fluorinated fraction. Because the dielectric constant varies linearly with density independent of the fluorine concentration, it is clear that the main contribution of the hexafluoroisopropylidene groups to lower dielectric properties is lower shrinkage and higher free volume and no other factors such as lower polarizability or hydrophobicity, as has been suggested in some previous studies. This finding also suggests that it should be possible to add other bulky groups, such as pendant phenyls, to the aerogel to increase the free volume and achieve the same results. Because fluorinated monomers are lower in reactivity and typically more expensive, this is a significant finding. However, the hierarchical pore structures that arise in the partially fluorinated aerogels may make them suitable for other applications, for example, acoustic absorbers, which require larger pores than those characteristically seen in aerogels.

■ AUTHOR INFORMATION

Corresponding Author

*E-mail: maryann.meador@nasa.gov.

Notes

The authors declare no competing financial interest.

■ ACKNOWLEDGMENTS

We thank the NASA Aeronautics Mission Directorate Seedling Fund for support of this work. We also thank Dan Scheiman and Linda McCorkle of the Ohio Aerospace Institute for analysis of the aerogels.

■ REFERENCES

(1) Volksen, W.; Miller, R. D.; Dubois, G. Low Dielectric Constant Materials. *Chem. Rev.* **2010**, *110*, 56−110.

(2) Hrubesh, L. W.; Keene, L. E.; Latorre, V. R. Dielectric Properties of Aerogels. *J. Mater. Res.* **1993**, *8*, 1736−1741.

(3) Meador, M. A. B.; Wright, S.; Sandberg, A.; Nguyen, B. N.; Van Keuls, F. W.; Mueller, C. H.; Rodríguez-Solís, R.; Miranda, F. A. Low Dielectric Polyimide Aerogels as Substrates for Lightweight Patch Antennas. *ACS Appl. Mater. Interfaces* **2012**, *4*, 6346−6353.

(4) Callus, P. J. Conformal Load-Bearing Antenna Structure for Australian Defense Force Aircraft. *Defense Science and Technology Report*; DSTO-TR-1963; file number 2006/1151925.

(5) Leflour, G.; Calnibalosky, C.; Jaquet, H. Reduction of Time and Costs for Antennas Integration Through Computational Electromagnetism. *Proceedings from NATO RTO-AVT Symposium on Reduction of Military Vehicle Acquisition Time and Cost through Advanced Modeling and Virtual Simulation*, Paris, France, April 22−25, 2002; pp 59-1−59-10.

(6) Chang, C.-J.; Tsai, M.-H.; Chen, G.-S.; Wu, M.-S.; Hung, T.-W. Preparation and Properties of Porous Polyimide Films with TiO_2/Polymer Double Shell Hollow Spheres. *Thin Solid Films* **2009**, *517*, 4966−4969.

(7) Jin, Y.; Tang, J.; Hu, J.; Han, X.; Shang, Y.; Liu, H. One Step Fabrication of Ultralow Dielectric Polyimide Films Consisting of Size-Controlled Mesoporous Nanoparticles. *Colloids Surf., A* **2011**, *392*, 178−186.

(8) Mochizuki, A.; Fukuoka, T.; Kanada, M.; Kinjou, N.; Yamamoto, T. Development of Photosensitive Porous Polyimide with Low Dielectric Constant. *J. Photopolym. Sci. Technol.* **2002**, *15*, 159−165.

(9) Carter, K. R.; DiPietro, R. A.; Sanchez, M. I.; Swanson, S. A. Nanoporous Polyimides Derived from Highly Fluorinated Polyimide/Poly(propylene oxide) Copolymers. *Chem. Mater.* **2001**, *13*, 213−221.

(10) Ren, Y.; Lam, D. C. Properties and Microstructures of Low Temperature Processable Ultralow Dielectric Porous Polyimide Films. *J. Electron. Mater.* **2008**, *37*, 955−961.

(11) Othman, M. B. H.; Ming, N. A. S.; Akil, H. M.; Ahmad, Z. Dependence of the Dielectric Constant on the Fluorine Content and Porosity of Polyimides. *J. Appl. Polym. Sci.* **2011**, *121*, 3192−3200.

(12) Ronova, I. A.; Bruma, M.; Schmidt, H.-W. Conformational Rigidity and Dielectric Properties of Polyimides. *Struct. Chem.* **2012**, *23*, 219−226.

(13) Simpson, J. O.; St. Clair, A. K. Fundamental Insight on Developing Low Dielectric Constant Polyimides. *Thin Solid Films* **1997**, *308−309*, 480−485.

(14) Hougham, G.; Tesoro, G.; Viehbeck, A.; Chapple-Sokol, J. D. Polarization Effects of Fluorine on the Relative Permittivity in Polyimides. *Macromolecules* **1994**, *27*, 5964−5971.

(15) Ye, Y.-S.; Chen, W.-Y.; Wang, Y.-Z. Synthesis and Properties of Low Dilectric Constant Polyimides with Introduced Reactive Fluorine Polyhedral Oligomeric Silsesquiozanes. *J. Polym. Sci., Part A: Polym. Chem.* **2006**, 5391−5402.

(16) Fricke, J. AEROGELS—Highly Tenous Solids with Fascinating Properties. *J. Non-Cryst. Solids* **1988**, *100*, 169−173.

(17) Meador, M. A. B.; Malow, E. J.; Silva, R.; Wright, S.; Quade, D.; Vivod, S. L.; Guo, H.; Guo, J.; Cakmak, M. Mechanically Strong, Flexible Polyimide Aerogels Cross-linked with Aromatic Triamine. *ACS Appl. Mater. Interfaces* **2012**, *4*, 536−544.

(18) Miranda, F. A.; Gordon, W. L.; Heinen, V. O.; Ebihara, B. T.; Bhasin, K. B. Measurements of Complex Permittivity of Microwave Substrates in the 20 to 300 K Temperature Range from 26. 5 to 40. 0 GHz. *NASA/TM 102123* **1989**.

(19) Brunauer, S.; Emmett, P. H.; Teller, E. Adsorption of Gases in Multimolecular Layers. *J. Am. Chem. Soc.* **1938**, *60*, 309−319.